

Supporting Material to
“Unscrambling Illusory Inhibition and Catalysis in Nanoparticle
Electrochemistry: Experiment and Theory”

Lifu Chen*, Enno Kätelhön*, and Richard G. Compton†

Department of Chemistry, Physical and Theoretical Chemistry Laboratory, Oxford
University, South Parks Road, Oxford, OX1 3QZ, United Kingdom

Contents

S1 Radius of the Diffusion Domain	2
S2 Experimental Details	4
S3 Stability of Carboxylated Polystyrene Microspheres	5
S4 Micrographs of Particle-Modified Electrodes	7
S5 Voltammetry at Bare Electrodes	8
S6 Peak-to-peak Separations for Multiple Layers of Polybead Microspheres	10
S7 Peak currents for Multiple Layers of Polybead Microspheres	11
S8 Voltammetry of Oxygen at Electrodes Modified with Nafion Microspheres	12

*Authors contributed equally.

†Corresponding author: Richard G. Compton, richard.compton@chem.ox.ac.uk

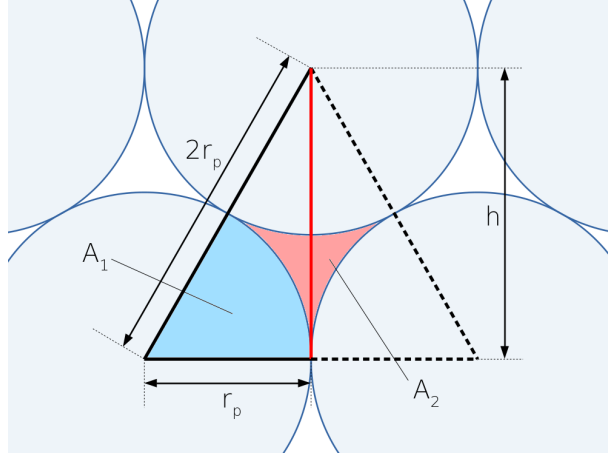


Figure S1: Illustration of the geometry considered in the approximation of the radius of the diffusion domain.

S1 Radius of the Diffusion Domain

To find an approximate value for the radius of the diffusion domain, we consider the two-dimensional projection of the first layer of spheres along an axis perpendicular to the electrode surface, see Figure S1, and determine the packing density η of the spheres in this projection. To this end, we consider an equilateral triangle, noting that the entire geometry can be constructed of such triangles and the packing density of spheres inside the boundaries of the triangle must hence equal the packing density in the entire structure. The length h can be calculated to:

$$h = \sqrt{(2r_p)^2 - (r_p)^2} = \sqrt{3} r_p \quad (\text{S1})$$

Using this value, we find that the total area A_{tot} of the triangle is:

$$A_{tot} = r_p h = \sqrt{3} (r_p)^2 \quad (\text{S2})$$

As evident from the figure, the area A_{tot} can be expressed through the total area occupied by spheres $3A_1$ and the unoccupied area A_2 :

$$A_{tot} = 3A_1 + A_2 \quad (\text{S3})$$

where we note that A_1 equals the area occupied by a sixth of a sphere:

$$A_1 = \frac{1}{6} \pi (r_p)^2 \quad (\text{S4})$$

Using the above results, the packing density η can be calculated to:

$$\eta = \frac{3A_1}{A_{tot}} = \frac{\frac{1}{2} \pi (r_p)^2}{\sqrt{3} (r_p)^2} = \frac{\pi \sqrt{3}}{6} = 0.9069 \quad (\text{S5})$$

The so-obtained packing density can now be implemented in the diffusion domain which sets the particle into the centre of a cylindrical space featuring the radius r_{max} . The electrode area occupied by a single

particle in the diffusion domain is hence:

$$A_p = \pi(r_p)^2 \quad (\text{S6})$$

while the total electrode area within the diffusion domain is:

$$A_{dd} = \pi(r_{max})^2 \quad (\text{S7})$$

The packing density within the diffusion domain can now be calculated and set to the value we determined above:

$$\eta = \frac{A_p}{A_{dd}} = \frac{\pi\sqrt{3}}{6} \quad (\text{S8})$$

which yields a value for the radius of the diffusion domain:

$$r_{max} = 1.0501 r_p \quad (\text{S9})$$

S2 Experimental Details

Chemicals

Polybead®Carboxylate Microspheres (carboxylated polystyrene, aqueous suspension, 2.5% solid content) of three different sizes ($0.5 \pm 0.004 \mu\text{m}$; $4.5 \pm 0.18 \mu\text{m}$; $20.0 \pm 2.27 \mu\text{m}$) were purchased from Polysciences (Germany). Ferrocenemethanol (FcCH_2OH , 97%, Santa Cruz Biotechnology), potassium chloride (KCl, $\geq 99.0\%$, Sigma-Aldrich), sodium chloride (NaCl, $\geq 99.5\%$, Sigma-Aldrich), sodium phosphate dibasic (Na_2HPO_4 , $\geq 99.0\%$, Sigma-Aldrich) and potassium phosphate monobasic (KH_2PO_4 , $\geq 99.0\%$, Sigma-Aldrich) were used as received without further purification. Nafion perfluorinated resin solution (5 wt% in lower aliphatic alcohol and water with a water content of 45%, Sigma-Aldrich) was heated in a water bath at $52 \pm 0.5^\circ\text{C}$ to obtain a concentrated 12.5wt% Nafion solution. Phosphate buffered saline buffer solution (PBS, pH = 7.4) was composed of 137 mM NaCl, 2.7 mM KCl, 10 mM Na_2HPO_4 and 1.8 mM KH_2PO_4 . All solutions were prepared using ultrapure water (Millipore) with a resistivity of not less than $18.2 \text{ M}\Omega \text{ cm}$ at 298 K and degassed with Argon before use.

Synthesis of Nafion Particles

Nafion particles were synthesized by the re-precipitation method. Briefly, 50 μL concentrated 12.5 wt% Nafion was injected dropwise over 10 seconds into 1 mL ultrapure water under stirring by magnetic vortexing at 600 rpm for 5 minutes. The resulting mixture was subjected to sonication (FB15050, Fisher Scientific, 50/60 Hz, Germany) for 30 min at room temperature. The suspension was then centrifuged (Eppendorf Centrifuge 5430 R) at 14000 rpm for 10 min and the precipitate was dispersed evenly in 0.5 mL water by sonication for 5 min. A stable suspension of sub-micron sized Nafion particles with an average radius of $0.43 \pm 0.26 \mu\text{m}$ [1, 2] was obtained.

Electrochemical Measurements

Electrochemical experiments were performed with an Autolab II potentiostat (Metrohm-Autolab BV, Netherlands) and a three-electrode set-up inside a grounded and thermostatted ($25.0 \pm 0.5^\circ\text{C}$) Faraday cage. A glassy carbon macroelectrode (GC, 3 mm diameter) was used as the working electrode, a saturated calomel electrode (SCE) as the reference electrode and a graphite rod as the counter electrode. Prior to each voltammetric scan, the working electrode was polished using micropolish alumina (Buehler) of decreasing particle size (1.0, 0.3 and $0.05 \mu\text{m}$) followed by sonication in water and drying with nitrogen. Varying amounts of the microspheres suspension were drop-casted on the GC macroelectrode to modify the electrode and left to dry under a nitrogen atmosphere. Cyclic voltammetry was conducted at selected scan rates of between 25 mVs^{-1} to 800 mVs^{-1} in 1.0 mM ferrocenemethanol supported with 0.1 M KCl.

For the study of Nafion particles, 10 μL of varying concentrations of fresh prepared Nafion particles suspension was drop-cast on the GC macroelectrode and left to dry under a nitrogen environment. The PBS buffer was placed in water bath at 25°C to for 1 h to obtain air saturated condition before measurements. Cyclic voltammetry was then conducted at selected scan rates of between 25 mVs^{-1} to 400 mVs^{-1} in air-saturated PBS buffer.

S3 Stability of Carboxylated Polystyrene Microspheres

We investigate the stability of the polybead microspheres in terms of possible swelling and shrinking under the utilised experimental conditions. To this end layers of polybead microspheres are subsequently dropcast centrally onto the electrode while the areas covered by each step decrease, hence forming three zones as seen in Figure S2a. A solution containing 1 mM ferrocenemethanol and 0.1 M KCl is slowly injected into the support cell and the electrode surface is immersed. Microscope images are taken after 20 min, which is the time scale for electrochemical experiments, and no change of the microspheres is observed as see Figure S2b. Finally, cyclic voltammetry is performed from -0.2 V vs. SCE to 0.6 V and back to -0.2 V at the scan rate of 25 mV s⁻¹ and a third micrograph is taken, see Figure S2c. Microspheres again remain visibly unaltered suggesting stability of the deposited layers throughout electrochemical experiments.

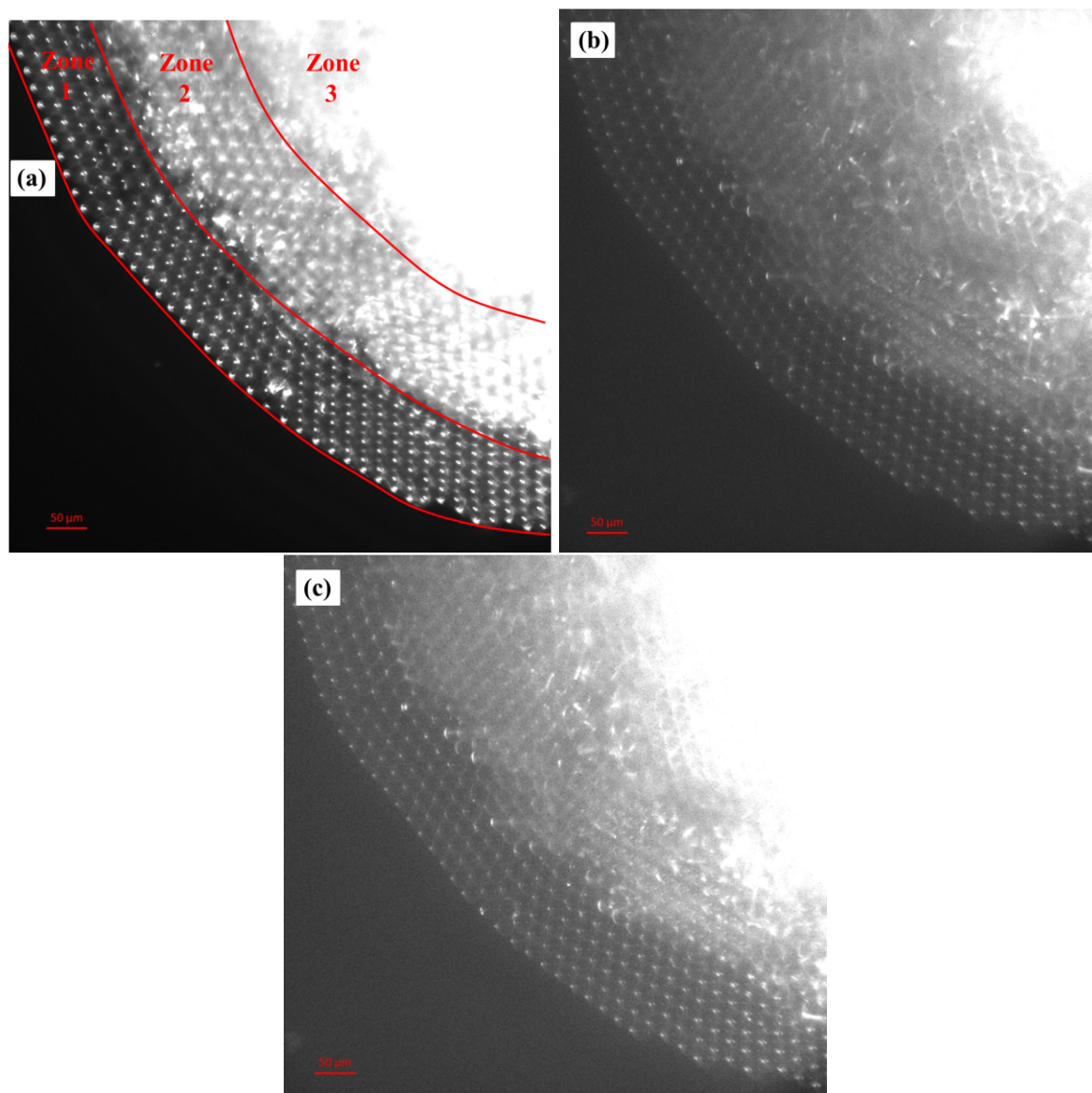


Figure S2: Optical microscope images of a glassy carbon macroelectrode modified with one layer (zone 1), two layers (zone 2) and multiple layers (zone 3) of polybead microspheres with 20 μm diameter (a) original microspheres after dried on the electrode surface (b) after immersion in solution containing 1mM ferrocenemethanol and 0.1 M KCl for 20 min (c) after a cyclic voltammetry from -0.2V vs. SCE to 0.6 V and back to -0.2V at the scan rate of 25 mV s^{-1} .

S4 Micrographs of Particle-Modified Electrodes

Figure S3 shows microscope images of a glassy carbon electrode modified with one layer of carboxylated polystyrene microspheres. A single-layer of spheres in a dense hexagonal packing can be seen locally though few black holes can be seen which feature sizes ranging from $5\ \mu\text{m}$ to $15\ \mu\text{m}$ and indicate that small areas of electrode surface have remained uncovered. It can be further noticed that the edge view of electrode surface shows rough outline in comparison with the larger microspheres.

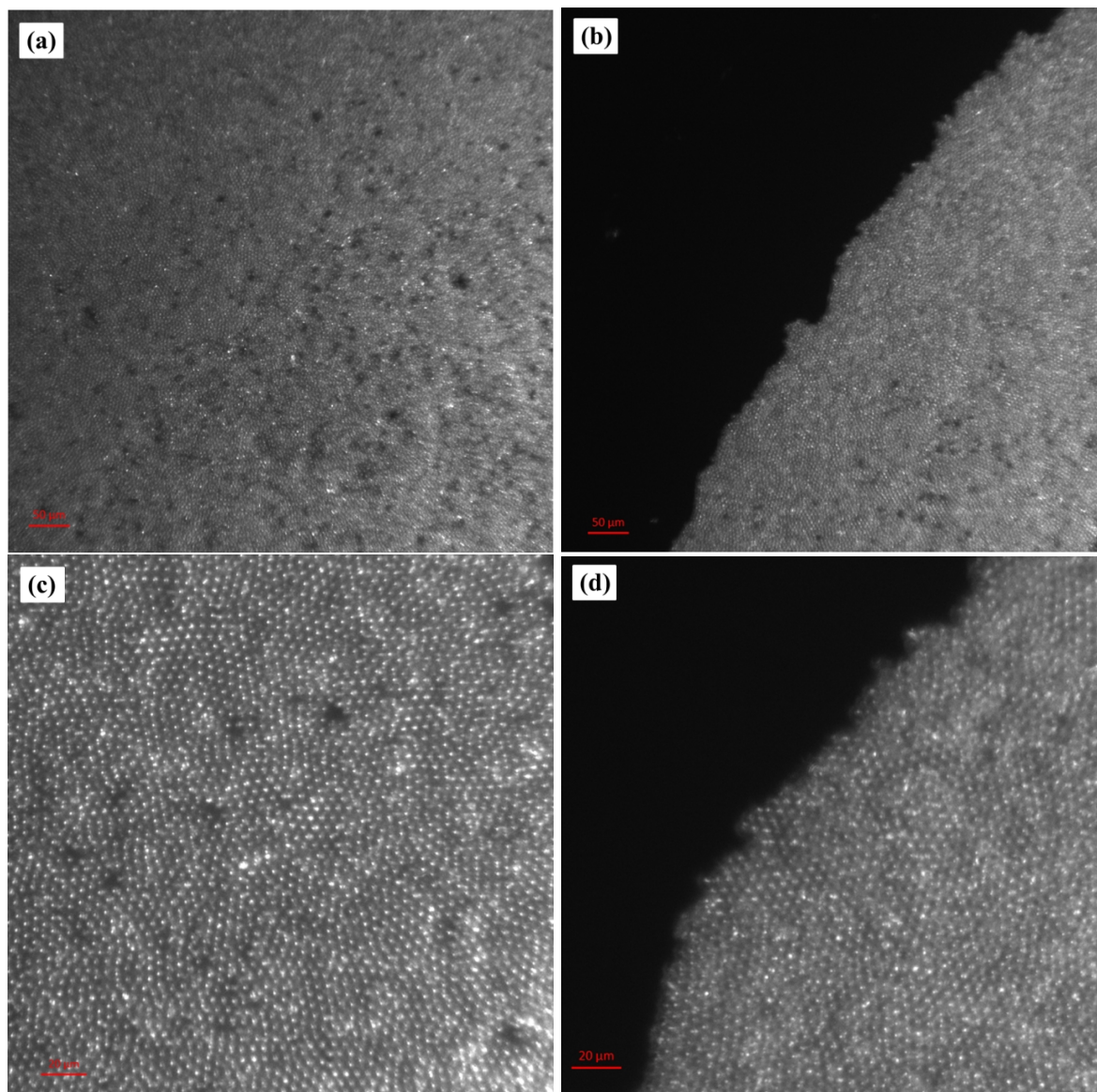


Figure S3: Micrographs of a glassy carbon macroelectrode modified with one layer of carboxylated polystyrene microspheres featuring a radius of $2.25\ \mu\text{m}$ (a) middle view of the electrode (b) edge view of the electrode (c) zoom-in of the middle view (d) zoom-in of the edge view.

S5 Voltammetry at Bare Electrodes

Figure S4 reveals that the peak current of ferrocenemethanol oxidation is directly proportional to the square root of the scan rate, suggesting the electrochemical reaction rate is diffusion limited. The diffusion coefficient of ferrocenemethanol can be determined via the one-electron-transfer, reversible Randles-Ševčík equation [3]:

$$I_p = 2.69 \cdot 10^5 A D^{\frac{1}{2}} C v^{\frac{1}{2}} \quad \text{at } 25^\circ\text{C} \quad (\text{S10})$$

where A is the geometrical surface area of working electrode, D is the diffusion coefficient, C is the concentration of the active species in the bulk solution, and v is scan rate. By this means the diffusion coefficient of ferrocenemethanol is calculated to be $7.6 \cdot 10^{-10} \text{ m}^2 \text{ s}^{-1}$, which is in excellent agreement with reported values, $(7.6 \pm 0.4) \cdot 10^{-10} \text{ m}^2 \text{ s}^{-1}$ [4]. The formal potential of ferrocene methanol oxidation can be approximated to be the mid-point potential of the voltammogram, which is about $190 \pm 1 \text{ mV}$ vs SCE.

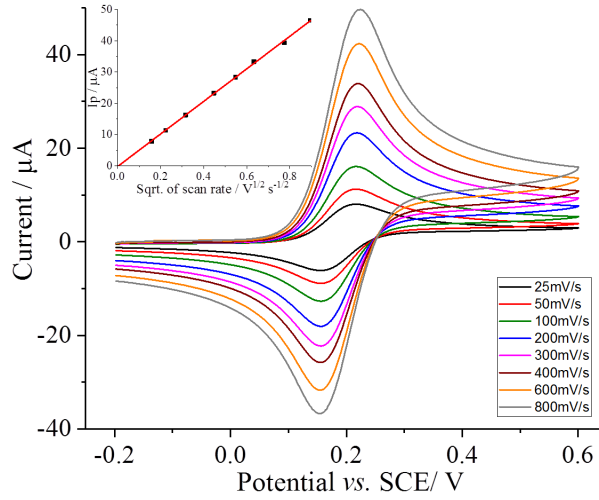


Figure S4: Voltammograms measured at a bare glassy carbon macroelectrode in a solution containing 1 mM ferrocenemethanol and 0.1 M KCl. The inset presents a plot of the peak current as a function of the square root of the scan rate.

The Figures S5 and S6 compare experimental and theoretical results for the peak-to-peak separations and peak currents, respectively. Good agreement is found for all data.

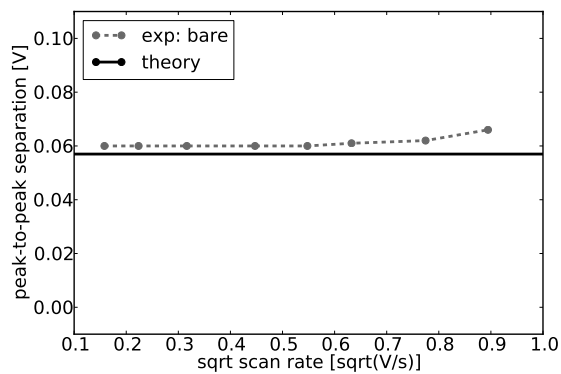


Figure S5: Comparison of measured and theoretical peak-to-peak separations as a function of scan rate. Experimental data was recorded in 1 mM ferrocenemethanol and 100 mM potassium chloride.

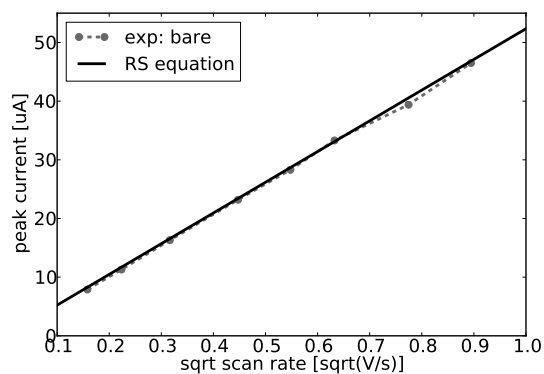


Figure S6: Comparison of measured, simulated, and theoretical peak currents as a function of scan rate. Theoretical peak heights are calculated via the Randles-Ševčík equation.

S6 Peak-to-peak Separations for Multiple Layers of Polybead Microspheres

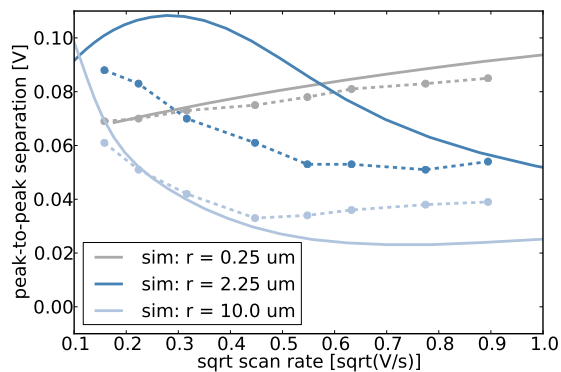


Figure S7: Comparison of measured (dashed lines) and simulated (solid lines) peak-to-peak separations as a function of scan rate for three different sizes of polybead microspheres and an average surface coverage of two layers of spheres. Experimental data was recorded in a solution comprising 1 mM ferrocenemethanol and 100 mM potassium chloride.

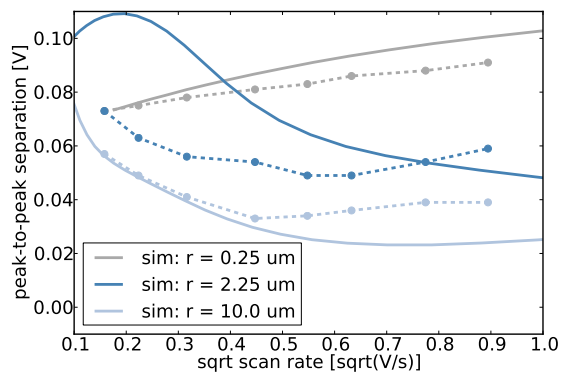


Figure S8: Comparison of measured (dashed lines) and simulated (solid lines) peak-to-peak separations for an average surface coverage of three layers of spheres. All other experimental details remain unchanged with regard to Figure S7

S7 Peak currents for Multiple Layers of Polybead Microspheres

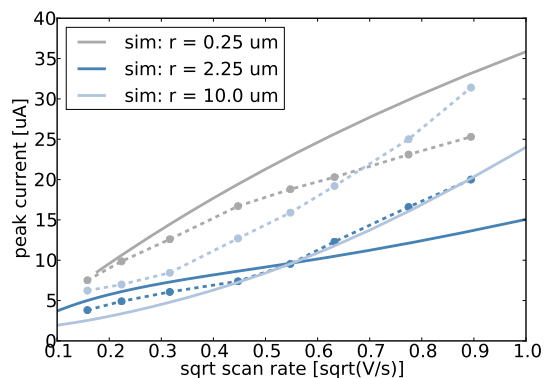


Figure S9: Comparison of measured (dashed lines) and simulated (solid lines) peak currents for an average of two layers of polybead microspheres. Experimental data was collected from the same voltammograms analysed in Figure S7.

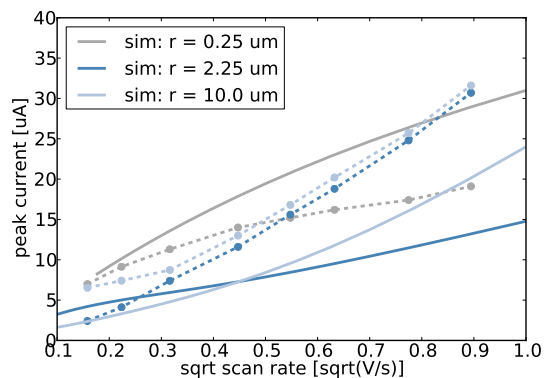


Figure S10: Comparison of measured (dashed lines) and simulated (solid lines) peak currents as a function of scan rate for an average of two layers of polybead microspheres. Data was collected from the raw data used in Figure S8.

S8 Voltammetry of Oxygen at Electrodes Modified with Nafion Microspheres

Figure S11 shows voltammograms measured at a bare and a Nafion-modified electrode in presence of oxygen and it can be seen that the Nafion particles seemingly ‘catalyse’ the oxygen reduction: The peak potential is lowered and the peak current higher while the Nafion particles themselves are inactive in the same solution as established above. We note that Nafion can increase the capacitance of carbon materials [5] which is consistent with the observation of the slight increase in the capacitive current in the presence of Nafion particles on the electrode (red line).

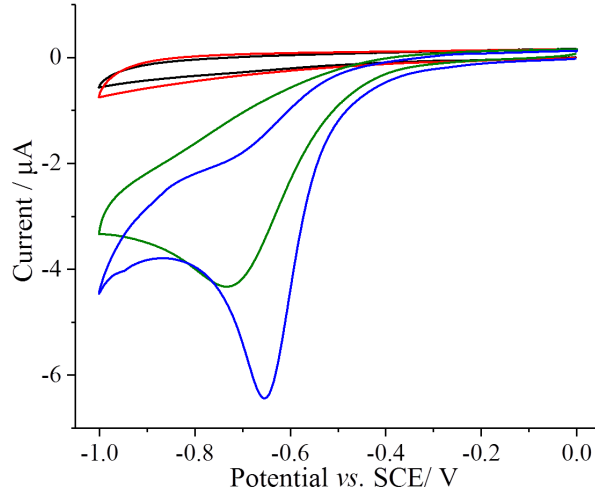


Figure S11: Voltammograms of a bare (black and green) and a modified (with 15 layers of Nafion particles, red and blue) glassy carbon macroelectrode in Argon-degassed PBS buffer solution at pH 7.4 and in air-saturated PBS buffer solution at pH 7.4. All voltammograms are recorded at a scan rate of 25 mV s⁻¹.

The diffusion coefficient of oxygen and the electrochemical transfer coefficient of the reaction are determined via the multiple-electron-transfer irreversible Randles-Ševčík equation [3]:

$$I_p = -0.496 \sqrt{n' + \alpha_{n'}} n F A C \sqrt{\frac{F v D}{RT}} \quad (\text{S11})$$

where n is the number of electrons transferred in the overall electrochemical process (here $n = 2$ for the reduction of oxygen to hydrogen peroxide [6]), n' is the number of electrons transferred before the rate determining step (here $n' = 0$ [7]), α is the apparent reductive transfer coefficient [8, 9], C is the oxygen concentration in solution (here $C = 0.26$ mM for an air-saturated solution [10]), F is the Faraday constant, R is the gas constant, and T is the temperature.

Figure S12a and S12b present voltammograms recorded at different scan rates and the corresponding Tafel plots. α is determined to be 0.25 via a Tafel analysis which is in good agreement with literature values [7]. The diffusion coefficient of oxygen in pH 7.4 aqueous solution is found to be $2.00 \cdot 10^{-9}$ m² s⁻¹, in an excellent agreement with the reported value of $1.95 \cdot 10^{-9}$ m² s⁻¹) [11].

The Tafel analysis was also performed for the voltammogram of a glassy carbon macroelectrode modified with 15 layers of Nafion particles and α has a value of 0.39, suggesting a relative faster electron

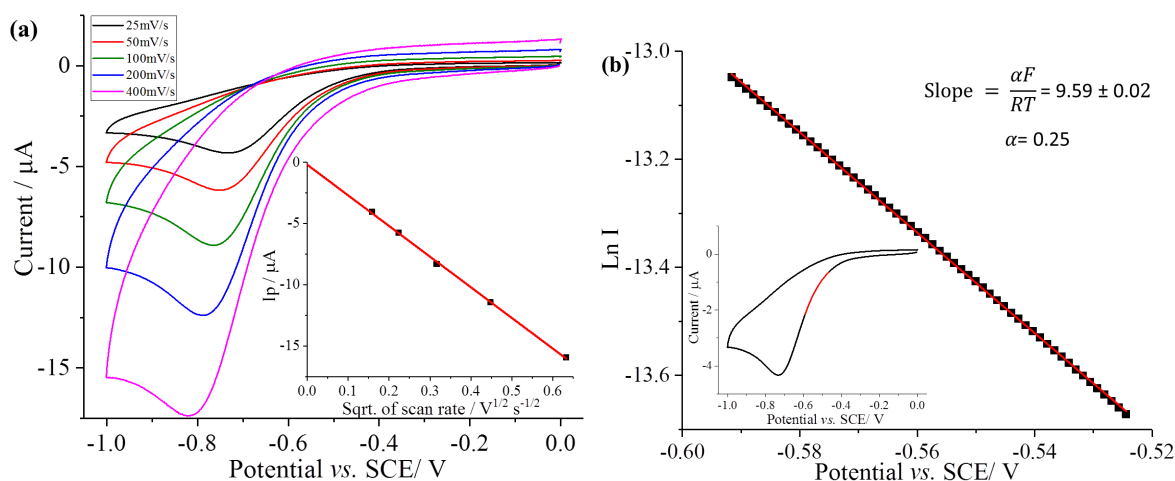


Figure S12: (a) Voltammograms of a bare glassy carbon macroelectrode in air-saturated pH 7.4 PBS buffer solution recorded for different scan rates. Inset: Plot of the peak current as a function of the square root of the scan rate. (b) Tafel analysis at a scan rate of 25 mV s⁻¹. The highlighted red region in the inset voltammogram is selected as the Tafel analysis region where the diffusion plays a near negligible role [12].

transfer (vs. $\alpha = 0.25$ for bare glassy carbon electrode).

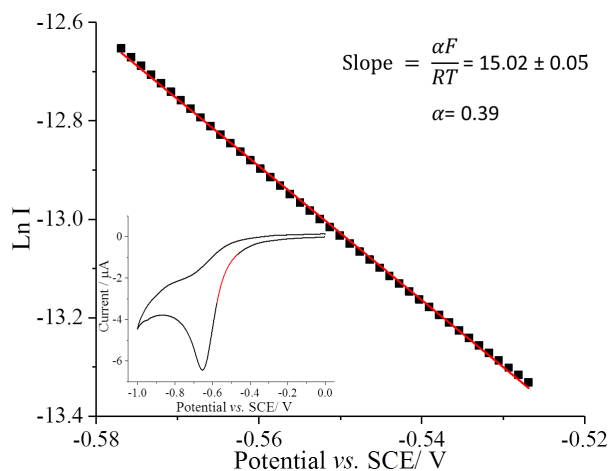


Figure S13: Tafel analysis for voltammogram of a glassy carbon macroelectrode modified with 15 layers of Nafion particles in air-saturated pH 7.4 PBS buffer at a scan rate of 25 mV s⁻¹. The highlighted red region in inset voltammogram was selected as the Tafel analysis region.

References

- [1] H. Yang, X. Li, C. Batchelor-McAuley, S. V. Sokolov, and R. G. Compton. Nafion particles doped with methyl viologen: electrochemistry. *Physical Chemistry Chemical Physics*, 20:682–689, 2017.
- [2] L. Chen, C. Lin, and R. G. Compton. Electrochemical characterisation and comparison of transport in Nafion films and particles. *Physical Chemistry Chemical Physics*, 21:607–616, 2019.
- [3] R. G. Compton and C. E. Banks. *Understanding Voltammetry (3rd Edition)*. World Scientific Press, 2018.
- [4] C. Amatore, N. Da Mota, C. Sella, and L. Thouin. Theory and Experiments of Transport at Channel Microband Electrodes under Laminar Flows. 1. Steady-State Regimes at a Single Electrode. *Analytical Chemistry*, 79:8502–8510, 2007.
- [5] F. Lufrano, P. Staiti, and M. Minutoli. Influence of Nafion Content in Electrodes on Performance of Carbon Supercapacitors. *Journal of The Electrochemical Society*, 151:A64–A68, 2004.
- [6] K. M. Sundberg, W. H. Smyrl, Lj. Atanasoska, and R. Atanasoski. Surface Modification and Oxygen Reduction on Glassy Carbon in Chloride Media. *Journal of The Electrochemical Society*, 136:434–439, 1989.
- [7] R. Nissim and R. G. Compton. Nonenzymatic Electrochemical Superoxide Sensor. *ChemElectroChem*, 1(4):763–771, 2014.
- [8] R. Guidelli, R. G. Compton, J. M. Feliu, E. Gileadi, J. Lipkowski, W. Schmickler, and S. Trasatti. Defining the transfer coefficient in electrochemistry: An assessment (IUPAC Technical Report). *Pure and Applied Chemistry*, 86:245–258, 2014.
- [9] R. Guidelli, R. G. Compton, J. M. Feliu, E. Gileadi, J. Lipkowski, W. Schmickler, and S. Trasatti. Definition of the transfer coefficient in electrochemistry (IUPAC Recommendations 2014). *Pure and Applied Chemistry*, 86:259–262, 2014.
- [10] R. E. Davis, G. L. Horvath, and C. W. Tobias. The solubility and diffusion coefficient of oxygen in potassium hydroxide solutions. *Electrochimica Acta*, 12:287–297, 1967.
- [11] L.-K. Ju and C. S. Ho. Measuring oxygen diffusion coefficients with polarographic oxygen electrodes: I. Electrolyte solutions. *Biotechnology and Bioengineering*, 27:1495–1499, 1985.
- [12] D. Li, C. Lin, C. Batchelor-McAuley, L. Chen, and R. G. Compton. Tafel analysis in practice. *Journal of Electroanalytical Chemistry*, 826:117–124, 2018.